Covalently linked hydrogen bond donors: The other side of molecular frustration in deep eutectic solvents

Cite as: J. Chem. Phys. 155, 084502 (2021); doi: 10.1063/5.0058165 Submitted: 27 May 2021 • Accepted: 6 August 2021 • Published Online: 24 August 2021







Elizabeth A. Recker, David Hardy, Grace I. Anderson, Arsalan Mirjafari, and Durgesh V. Wagle 🗓



AFFILIATIONS

Department of Chemistry and Physics, Florida Gulf Coast University, 10501 FGCU Blvd. S., Fort Myers, Florida 33965, USA

Note: This paper is part of the JCP Special Topic on Chemical Physics of Deep Eutectic Solvents.

a) Author to whom correspondence should be addressed: dwagle@fgcu.edu

ABSTRACT

In this work, we investigated the effects of a single covalent link between hydrogen bond donor species on the behavior of deep eutectic solvents (DESs) and shed light on the resulting interactions at molecular scale that influence the overall physical nature of the DES system. We have compared sugar-based DES mixtures, 1:2 choline chloride/glucose [DES_(g)] and 1:1 choline chloride/trehalose [DES_(t)]. Trehalose is a disaccharide composed of two glucose units that are connected by an α -1,4-glycosidic bond, thus making it an ideal candidate for comparison with $glucose\ containing\ DES_{(g)}.\ The\ differential\ scanning\ calorimetric\ analysis\ of\ these\ chemically\ close\ DES\ systems\ revealed\ significant\ difference$ in their phase transition behavior. The DES(g) exhibited a glass transition temperature of -58 °C and behaved like a fluid at higher temperatures, whereas $DES_{(t)}$ exhibited marginal phase change behavior at $-11\,^{\circ}C$ and no change in the phase behavior at higher temperatures. The simulations revealed that the presence of the glycosidic bond between sugar units in DES(t) hindered free movement of sugar units in trehalose, thus reducing the number of interactions with choline chloride compared to free glucose molecules in DES(g). This was further confirmed using quantum theory of atoms in molecule analysis that involved determination of bond critical points (BCPs) using Laplacian of electron density. The analysis revealed a significantly higher number of BCPs between choline chloride and sugar in DES_(g) compared to DES_(t). The $DES_{(g)}$ exhibited a higher amount of charge transfer between the choline cation and sugar, and better interaction energy and enthalpy of formation compared to DES_(t). This is a result of the ability of free glucose molecules to completely surround choline chloride in DES_(g) and form a higher number of interactions. The entropy of formation for DES(t) was slightly higher than that for DES(g), which is a result of fewer interactions between trehalose and choline chloride. In summary, the presence of the glycosidic bond between the sugar units in trehalose limited their movement, thus resulting in fewer interactions with choline chloride. This limited movement in turn diminishes the ability of the hydrogen bond donor to disrupt the molecular packing within the lattice structure of the hydrogen bond acceptor (and vice versa), a crucial factor that lowers the melting point of DES mixtures. This inability to move due to the presence of the glycosidic bond in trehalose significantly influences the physical state of the DES(t) system, making it behave like a semi-solid material, whereas DES(g) behaves like a liquid material at room temperature.

Published under an exclusive license by AIP Publishing. https://doi.org/10.1063/5.0058165

INTRODUCTION

Deep eutectic solvents (DESs) were first introduced by Abbott in 2004, a leading innovator in the field, who reported that mixing a high melting organic salt, a hydrogen bond acceptor (HBA), and a neutral organic molecule, a hydrogen bond donor (HBD), in appropriate molar ratio results in a mixture that is a liquid at room temperature.^{1,2} For instance, mixing a high melting organic quaternary ammonium salt such as choline chloride (m.p. = 302 °C) and a high melting organic molecule such as urea (m.p. = 133 °C) in appropriate mole ratio (1:2 mole ratio of choline chloride and urea) results in a eutectic mixture that is liquid at room temperature (m.p. = 32 °C). Since their inception, several DES formulations have been developed by pairing choline chloride with amides, carboxylic acids, glycols, phenols, and sugars—offering flexibility in the chemical composition to allow for designing DESs suitable for specific application. DESs have been touted as modern and greener alternatives to ionic liquids and volatile organic solvents, mostly due

to the nontoxic, biological origin of the starting materials that are employed to make DESs, for example, choline chloride, urea, carboxylic acids, and sugars, to name a few. ¹⁻⁵ Apart from the zero waste nature of their synthesis and low toxicity, DESs generally have several advantageous properties, such as negligible volatility, wide electrochemical window, broad liquid range, strong solvating ability for a wide range of organic and inorganic compounds, and excellent recyclability. ^{1,6-8} These qualities allow for utilization of DESs in various applications, including biomass treatment, ⁹ catalysis, electrochemistry, functional materials, ¹⁰ gas separation, ^{11,12} synthesis of nanomaterials, ¹³⁻¹⁵ micelle formation, ¹⁶ and polymer synthesis. ¹⁷

Due to the growing interest in the utility of DESs in a wide variety of applications, it has become imperative to understand their molecular structure and dynamics in order to tailor them for a specific application. In recent years, there have been several experimental and computational studies that are focused on understanding their structure and dynamic nature on a fundamental molecular level. In fact, the field of deep eutectics has witnessed a significant rise in the experimental work on a wide variety of DESs. 18-20 However, there have been far fewer computational studies, primarily focused on understanding the common types of DESs, such as choline chloride/urea and choline chloride/ethylene glycol.²¹ Molecular dynamics (MD) simulations by Sun et al. on choline chloride- and urea-based DESs revealed that the disruption in the long-range ordering of choline chloride by urea, increase in the hydrogen-bonding lifetimes between urea and Cl- anion, and significant moderation in urea-urea and choline-chloride interaction energies resulted in substantial depression in the melting points for the DES mixtures.²² This is in corroboration with the work carried out by Hammond et al., indicating the formation of a layered structure in reline due to the significant contribution of the hydroxyl group of choline in the bonding network.²³ Similarly, Perkins et al. made observations using MD simulations and infrared spectroscopy that DES components prefer molecular orientation that promote a maximum number of hydrogen bonds between HBDs and Cl⁻, resulting in the low-melting nature of the DES.²⁴ Our earlier work on choline chloride-/glycerol-based DES using neutron scattering experiments and quantum chemical simulations indicated higher translational diffusion of the choline cation compared to glycerol. This higher translational diffusion of glycerol arises from its ability to form multiple hydrogen bonds with the Cl⁻ anion.²⁵ The work by García et al. using density functional theory (DFT) simulations provided an insight into a linear relationship between the variation in the electron density at the cage critical points of the hydrogen-bonding interactions and melting temperatures of choline-based DES systems.²⁶ Quantum chemical calculations by Rimsza and Corrales on reline containing Cu and CuO indicated charge transport occurring through proton hopping in the DES.²⁷ Zhang et al. provided an experimental and quantum chemical insight into the role of choline chloride-/magnesium chloride hexahydrate-based DES in electrochemical deposition of magnesium chloride.²⁸ Although there is a significant amount of research available on studying DESs through simulations, most of the studies are focused exclusively on simple eutectic mixtures that involve molecules in monomeric forms. However, there are a few studies that are focused on molecules such as di-cations, di-anions, or neutral species that exist as dimers which can potentially form deep eutectic mixtures.

In this work, we have investigated the influence of a single covalent bond link between HBD species on behavior of DESs and shed light on the interactions at molecular scale that influence the physical nature of the DES system. Herein, we have compared 1:2 choline chloride/glucose [DES $_{(g)}$] and 1:1 choline chloride/trehalose [DES $_{(t)}$] systems (Fig. 1). Trehalose is a disaccharide composed of two glucose units that are connected by a 1,4-glycosidic bond between C1 carbon of one glucose unit and C4 carbon of the second sugar unit, making it ideal for comparison with DES(g) that contains free glucose units. It should be noted that the aforementioned DES systems do not represent the eutectic mixtures with lowest melting points. These molar ratios of choline chloride to sugar in $DES_{(g)}$ (1:2) and $DES_{(t)}$ (1:1) were picked to maintain equal number of monomeric sugar units for direct comparison between the two DES systems to study the effects of a covalent link between sugar units on interactions with choline chloride. Furthermore, since the trehalose is a dimeric sugar that contains two glucose units, the use of other molar ratios for choline chloride to trehalose, such as 1:3, 1:4, 2:1, and 2:3, would significantly add to the computational cost. Therefore, a small representative cluster of choline chloride and sugar has been used in this study to maintain a reasonable computational

In liquids, characterization of properties such as melting $\left(T_{m}\right)$ and glass transition $\left(T_{g}\right)$ points is crucial since these properties are the manifestations of the underlying molecular interactions at atomic and bulk scales. In this work, we performed the

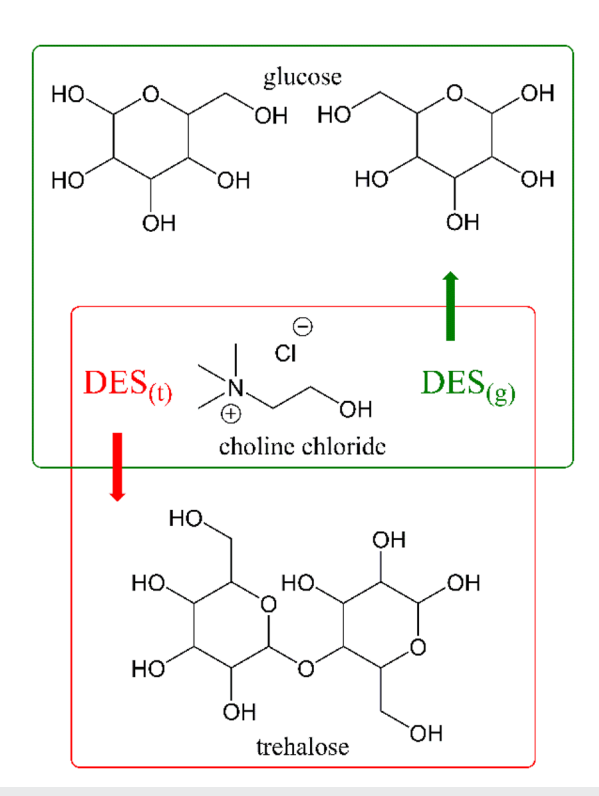


FIG. 1. Scheme illustrating the two DES systems studied in this work. $DES_{(g)}$ and $DES_{(t)}$ represent glucose- and trehalose-based DES systems, respectively.

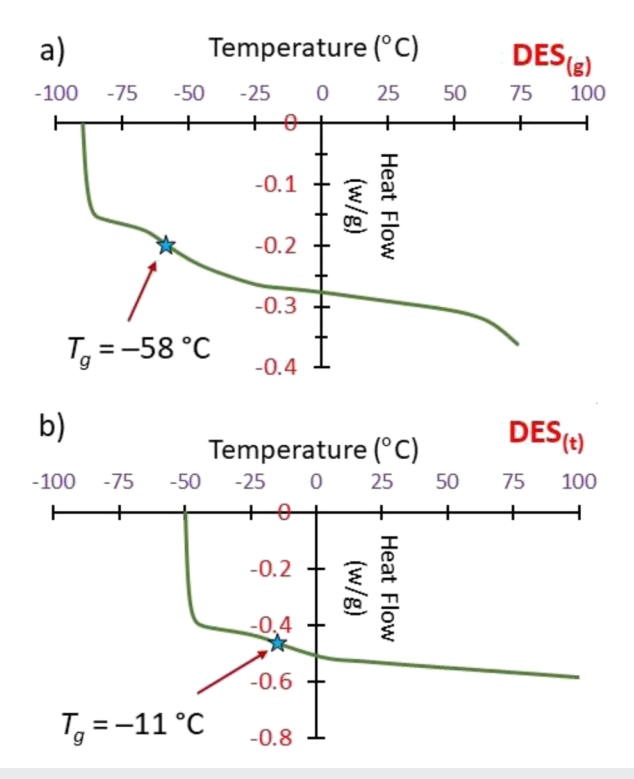


FIG. 2. Comparison between differential calorimetric analysis of DES systems: (a) $DES_{(j)}$ and (b) $DES_{(j)}$.

Differential Scanning Calorimetric (DSC) analysis of the DES systems and observed that both the systems exhibited glass transition behavior. The effect of covalently linking the sugar molecules through the glycosidic bond can be clearly observed in DES(t) by monitoring the phase change behavior of these chemically close DES systems during (DSC) analysis. The heating cycle of the DSC analysis for DES_(g) revealed a gradual drop in the heat flow of about 0.11 w/g between -78 and -38 °C with glass transition point (T_g) at -58 °C, whereas for DES(t), a gradual drop in the heat flow of about 0.11 w/g between -30 and 10 °C with T_g value of -11 °C was observed (Fig. 2). Furthermore, at temperatures >50 °C, DES_(g) exhibited a significant change in the heat flow of about 0.5 w/g, an indication of fluid-like behavior, whereas DES(t) had no drastic change in the heat flow at elevated temperature >75 °C. As evident from the DSC analysis, it is interesting to note that a small change, such as covalently linking HBDs, can lead to a significantly different behavior in chemically similar DES systems. To understand the underlying factors influencing the behavior of the DES system, we turned our attention to quantum chemical simulations to get an atomistic insight into the molecular interactions in the DES system.

EXPERIMENTAL METHODS

A detailed description of materials, synthesis, characterization, and instrumentation used in this work can be found in the supplementary material.

COMPUTATIONAL METHODS

The optimization of the DES clusters was carried out by employing various initial orientations of the choline chloride around HBD molecules in which choline chloride was sandwiched between HBD molecules or it was placed in-plane or out-of-plane with respect to HBD molecules (see Figs. S1 and S2 in the supplementary material). The preliminary optimization of these starting orientations was performed at HF/6-31G(d,p) level of theory and was followed by reoptimization, and thermochemistry was carried out at the higher M06-2X/6-31++G(d,p) level using keywords opt and freq.²⁹ All simulations were carried out with no symmetry restrictions in the singlet ground state. The Boys and Bernadi counterpoise procedure was used to account for basis set superposition error (BSSE) using the keyword counterpoise=cp.³⁰ The dispersion correction in the M06-2X calculations was taken into account for the thermochemistry of DES formation using the method developed by Grimme.³¹ The atomic charges were obtained using electrostatic potential maps using the grid-based method (CHELPG) at M06-2X using the keyword pop=CHELPG. All calculations reported here were carried out using the Gaussian 16W software package.³² The absence of imaginary frequencies in the computed structures indicated that the optimized structures were minimum. Quantum Theory of Atoms In Molecules (QTAIM) analysis was carried out using the Multiwfn-a multifunctional wavefunction analyzer software package.³³ Thermochemical values for the optimized DES clusters were obtained using the following equation:

$$\Delta X_{DES} = X_{DES} - X_{ChCl} - nX_{HBD}$$
.

Here, X is the BSSE-corrected enthalpy (H), or entropy (S), or free energy (G), or interaction energy (E), where n = 1 (trehalose) or 2 (glucose). The molecules were visualized using GaussView 6.0.16. The examples of the input files used to perform the simulations are provided in the supplementary material.

RESULTS AND DISCUSSION

Geometry

Computational chemistry provides a valuable insight into understanding the structures and orientations of various DES components and their interactions within DES systems. A comprehensive analysis of weak molecular interactions, such as van der Waals forces, hydrogen bonding, electrostatic interactions, and strong interactions (i.e., covalent bonds) are crucial to understand the factors that influence the physical properties of a system, such as melting point, viscosity, surface tension, and thermal stability. In this study, the structures of glucose- and trehalose-based DESs were optimized using the M06-2X/6-31++G(d,p) method and basis set. This method and the basis set were calibrated in our earlier work through comparison of the structure and thermodynamic properties of the DES system with M06-2X/aug-cc-pVDZ, MP2/aug-cc-pVDZ, and MP2/6-31++G(d,p) levels of theory.³⁵ The M06-2X/6-31++G(d,p) method and basis set consistently predicted the structure and thermodynamic properties compared to other methods, thus confirming the reproducibility and reliability of the results under consideration.

The comparison between the DES clusters that contain monosaccharide and disaccharide sugars as HBDs renders the ability to study the influence of a single covalent bond (glycosidic link) between HBD molecules on the physical properties of the sugarbased DES. It is already a well-established phenomenon that the formation of DES is a result of disruption of interactions between molecules of same species by another species that breaks down the crystal lattice structure.²² This ability of one molecular species to disturb the lattice structures of another species is derived from the extent to which a molecule can move freely. In DES_(t), it was observed that the presence of a single glycosidic bond between the sugar units in trehalose significantly restricted the movement of the sugar units in the DES, whereas in DES(g), the absence of this glycosidic link enabled the sugar units to move freely and allowed choline chloride to sandwich between sugar molecules and disrupt the interactions between the sugar units [Fig. 3(a)]. The glycosidic bond in trehalose acts like a hinge that prevents trehalose from opening up wide enough to accommodate choline chloride [Fig. 3(b)]. The noncovalent interaction distances between molecular species are another indicator for the strength of interaction between the organic salt and sugars. The optimized structures indicated a higher number of interactions between sugar and choline chloride units in DES(g) compared to DES_(t). In DES_(g), the methyl protons on the ammonium head of the choline cation interacted with the oxygen atoms of the -OH groups of sugar at distances of 2.313 and 2.349 Å, whereas in $DES_{(t)}$, the distance was 2.259 Å for such a single interaction. Moreover, the hydroxyl tail of the choline cation formed two hydrogen bonding interactions with the sugar units in $DES_{(g)}$, whereas in DES(t), it was involved in a single hydrogen bonding with Cl-. The higher number of interactions in DES_(g) compared to DES_(t) arises from the ability of sugar molecules in DES(g) to move freely and encircle choline chloride. The optimized structures also revealed that the Cl- had a significantly higher number of interactions with choline and sugars in DES(g) relative to DES(t). The Cl- interacted with three methyl protons of the ammonium group of choline at interaction distances ranging between 2.444 and 2.573 Å, whereas in DES_(t), the Cl⁻ interacted with the methylene (-CH₂-) proton in the tail of the choline cation, with an interaction distance of 2.655 Å. The higher number of interactions in $\ensuremath{\mathsf{DES}}_{(g)}$ allowed for the formation of a transient cage-like structure, an important feature of DESs that

was previously observed in common DES mixtures, such as reline, ethaline, and glycline.^{24–26} From the analysis of the optimized structures of DESs, it is evident that the glycosidic link between the sugar units in DES(t) significantly reduces the ability of the molecule to move freely, thus reducing the number of interactions with choline chloride. These effects of reduction in interactions in the DES on the physical behavior of the DES can be observed in the DSC analysis of the two DES systems. The heating cycle of the DSC analysis for $DES_{(g)}$ revealed a gradual drop in the heat flow of about 0.11 w/g between -78 and -38 °C with the glass transition point (T_g) at -58 °C, whereas for DES_(t), a gradual drop in the heat flow of about 0.11 w/g between -30 and $10\,^{\circ}$ C with T_g at $-11\,^{\circ}$ C was observed. Furthermore, at temperatures >50 $^{\circ}\text{C}$, DES $_{(g)}$ exhibited a significant change in the heat flow of about 0.5 w/g, an indication of fluid-like behavior, whereas DES(t) had no drastic change in the heat flow at elevated temperature >75 $^{\circ}$ C.

Charge transfer

Charge transfer between molecules occurs through perturbation and redistribution of electron density when two molecules come in contact with each other. The quantitative analysis of this redistribution of electron density accounts for the amount of charge transfer that occurs between molecules and provides an insight into the strength of the interaction. It was observed that, in DESs, there was no significant change in the charge of the Cl⁻ anion, while the choline cation gained more positive charge in DESs compared to the choline cation in the free choline chloride and the sugar molecules gained more negative charge compared to free sugar (Table I). This indicates that the charge transfer is occurring from the choline cation to sugar molecules in the DES clusters, a trend observed in other choline chloride-based DESs. 35 Interestingly, it was observed that the amount of charge transfer from the choline cation to glucose was -0.11139e in DES(g), which is almost twice as high compared to DES_(t) with a net gain in charge of $-0.067~89e^-$ for trehalose

This trend in the charge transfer process between the choline cation and sugar is in corroboration with the higher number of interactions between the choline cation and glucose in $\mathrm{DES}_{(g)}$ compared to interactions between the choline cation and trehalose in

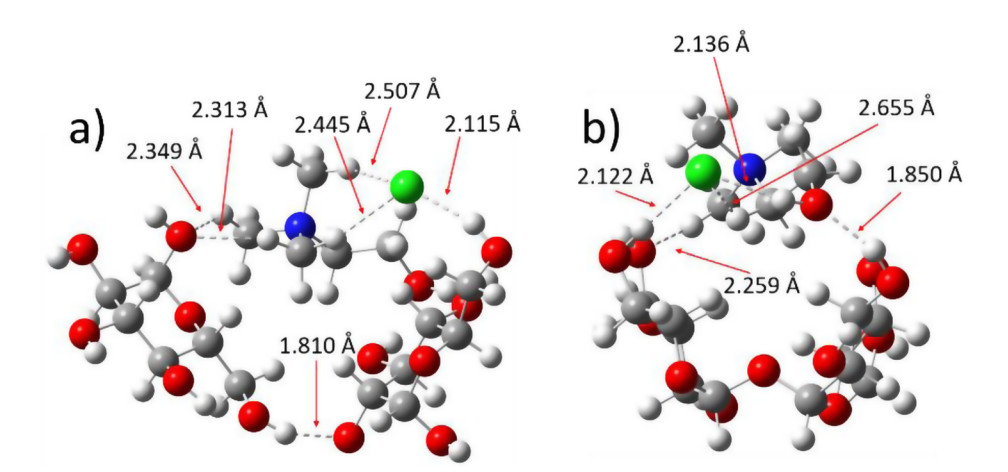


FIG. 3. Optimized geometries of the DES clusters at M06-2X/6-31++G(d,p) level of theory depicting interaction distances:
(a) DES_(g) containing choline chloride/glucose (1:2) and (b) DES_(t) containing choline chloride/trehalose (1:1).

TABLE I. CHELPG charges on choline chloride and HBDs (glucose and trehalose) before and after formation of DES mixtures.

	Glucose	Trehalose	Choline	Chloride
Free DES _(g) DES _(t)	0.0 -0.111 39	0.0 -0.067 89	0.762 74 0.875 25 0.829 47	-0.76274 -0.76387 -0.76157

DES_(t). The optimized structures revealed that in DES_(g), along with two strong hydrogen bonds between the hydroxyl tail of the choline cation and glucose, there were interactions between three methyl groups (-CH₃) of the ammonium on the choline cation and hydroxyl groups of glucose, whereas in $\text{DES}_{(t)}$, trehalose interacted with a single methyl group on the ammonium head of the choline cation and formed one hydrogen bond with the hydroxyl tail of the choline cation. The higher number of interactions between glucose and the choline cation allows for efficient charge transfer between the species in $\text{DES}_{(g)}$. Maximizing the interactions between different species and minimizing the interaction between same species is the driving force for formation of DESs. The charge transfer analysis indicates that the single glycosidic bond between the sugar units in trehalose hindered the free movement of sugar units and prevented them from surrounding choline chloride, leading to fewer interactions and lower charge transfer between the species in $DES_{(t)}$.

Although the charge transfer process between the various components of the DESs provides an insight into their interactions through estimation of electron density (ρ) redistribution, it provides no information about the ρ maxima consistent with the electron pairs of the Lewis model when two atoms interact with each other. Therefore, it is crucial to perform QTAIM analysis that involves determination of BCPs by estimating the Laplacian of electron density ($\nabla^2 \rho$) to pinpoint those interactions. The BCP is a point on a ridge of an electron density map between two interacting atoms where electron density distribution [ρ (r)] is minimum, typically termed as (3, -1) type BCP or "a saddle point in the electron density between two atoms." The QTAIM analysis of the two optimized DES clusters revealed a significantly higher number of BCPs

TABLE II. The Laplacian of the electron density at the BCP of interactions between various components in the DES clusters, where Ch is choline, G is glucose, and T is trehalose.

DES _(g)		DES _(t)		
BCP of interaction	$(\nabla^2 \rho)$	BCP of interaction	$(\nabla^2 \rho)$	
$G(OH) \cdots G(OH)$	0.111	$T(OH) \cdot \cdot \cdot Cl^{-}$	0.716	
$G(CH_2) \cdot \cdot \cdot G(OH)$	0.1866	$Ch(CH_2)\cdots T(OH)$	0.1617	
$Ch(CH_3) \cdot \cdot \cdot G(OH)$	0.2426	$Ch(CH_2)\cdots T(OH)$	0.2651	
$Ch(CH_3) \cdot \cdot \cdot G(-O-)$	0.1718	$Ch(CH_3)\cdots T(OH)$	0.4569	
$Ch(CH_3) \cdot \cdot \cdot G(OH)$	0.2471	$Ch(CH_3)\cdots T(OH)$	0.3282	
$Ch(CH_3) \cdot \cdot \cdot G(OH)$	0.1903	$Ch(CH_3)\cdots T(OH)$	0.3165	
$Ch(CH_2) \cdot \cdot \cdot G(OH)$	0.2061	$Ch(CH_3)\cdots Cl^-$	0.7055	
$Ch(CH_2) \cdot \cdot \cdot G(OH)$	0.2774	$Ch(CH_3)\cdots T(CH)$	0.2646	
$Ch(CH_3) \cdot \cdot \cdot G(-O-)$	0.4258	$Ch(CH_2) \cdot \cdot \cdot Cl^-$	0.1442	
$G(OH) \cdot \cdot \cdot Cl^{-}$	0.7133	$Ch(CH_3)\cdots T(CH)$	0.4229	
$G(CH) \cdot \cdot \cdot Ch(OH)$	0.3385	$T(CH) \cdot \cdot \cdot Ch(OH)$	0.4193	
$-CH_3 \cdot \cdot \cdot G(-O-)$	0.3246	$Ch(CH_2)\cdots T(OH)$	0.3346	
$Ch(CH_2) \cdot \cdot \cdot G(OH)$	0.349	$T(OH) \cdot \cdot \cdot Ch(OH)$	0.1008	
$Ch(CH_3)\cdots Cl^-$	0.4901	$Ch(CH_2)\cdots T(OH)$	0.4786	
$Ch(OH) \cdot \cdot \cdot G(OH)$	0.8536	$Ch(CH_3) \cdot \cdot \cdot Cl^-$	0.2515	
$Ch(CH_2) \cdot \cdot \cdot G(OH)$	0.4333			
$Ch(OH) \cdot \cdot \cdot G(OH)$	0.9089			
$Ch(CH_3) \cdot \cdot \cdot G(OH)$	0.429			
$Ch(CH_2) \cdot \cdot \cdot Cl^-$	0.4284			
$Ch(CH_3)\cdots Cl^-$	0.4477			

between the choline cation, chloride anion, and sugar in $DES_{(g)}$ compared to the $DES_{(t)}$ (Fig. 4). This quantitative analysis confirms the higher number interaction between various components in $DES_{(g)}$ compared to $DES_{(t)}$ is in good agreement with previously made observations discussed in the section titled Geometry.

Table II lists the Laplacian of the electron density $(\nabla^2 \rho)$ at the BCP for various inter-molecular interactions between different species within the DES clusters. It clearly depicts the significant disparity in the number of interactions that involve the choline cation and the sugar in the DES clusters with the higher number of interactions in DES_(g) compared to DES_(t). This higher number of interactions between the choline cation and glucose in DES_(g) significantly

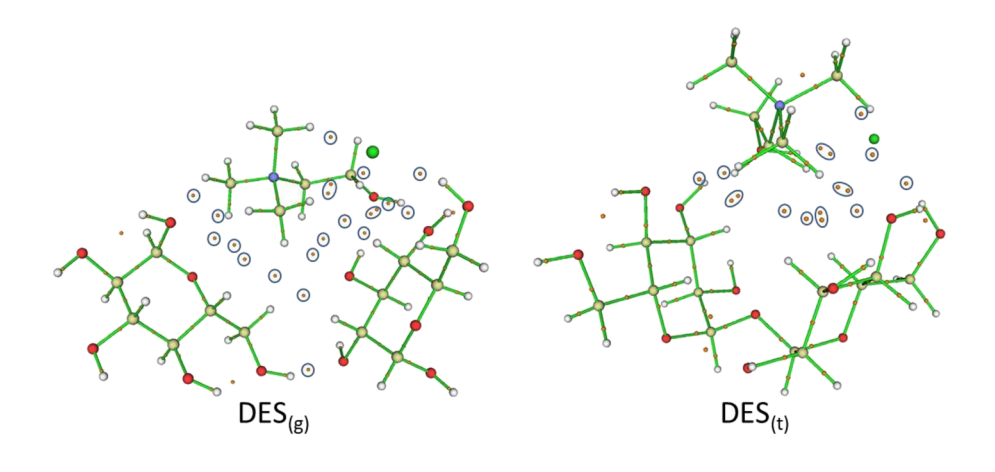


FIG. 4. QTAIM analysis of the optimized geometries of the DES clusters at M06-2X/6-31++G(d,p) level of theory depicting bond critical points (BCPs) between choline chloride and sugar molecules that have been highlighted by blue circles and ovals

TABLE III. Change in the free energy, enthalpy, interaction energy, and entropy associated with formation of the DES mixtures.

	ΔG (kcal/mol)	ΔH (kcal/mol)	ΔE (kcal/mol)	Δs (kcal/mol)
DES _(g)	-9.43	-35.81	-39.70	-0.088
DES _(t)	-12.07	-26.51	-28.57	-0.048

disrupts the glucose–glucose interactions. Unlike $DES_{(t)}$, the higher number of interactions in $DES_{(g)}$ is a direct consequence of the ability of the glucose molecules to move around due to the absence of the glycosidic bond between sugar molecules.

Thermochemistry

We observed that free energy (ΔG), enthalpy (ΔH), and total energy (ΔE) of formation for the DESs are significantly negative, indicating that the formation of these DESs is a favorable process. Interestingly, ΔG is more favorable for DES_(t) compared to DES_(g) by 2.65 kcal/mol, whereas ΔH and ΔE of formation for DES_(g) were significantly lower than for DES(t) by 9.30 and 11.13 kcal/mol, respectively. This indicates that, although the formation of DES(t) is a slightly more favorable process, more heat is released during the formation of DES_(g) as the glucose units are free to move, leading to the higher number of interactions with choline chloride, whereas the glycosidic bond in trehalose restricts its movement and reduces its interactions with choline chloride. There is a marginal entropic penalty upon formation of DESs with entropic values for DES(g) and DES_(t) at -0.089 and -0.048 kcal/mol, respectively (Table III), indicating the favorable interaction between various components of DESs. A slightly higher value of entropy for DES_(t) compared to $DES_{(g)}$ is attributed to the rigidity in the trehalose that arises from the hinge-like α -1,4-glycosidic bond between the sugar units of the trehalose. This hinge-like bond hinders the ability of glucose units of trehalose to surround choline chloride and form tighter hydrogen bond interactions with Cl-, as discussed earlier in the section titled Geometry. Unlike DES_(t), in DES_(g) the absence of the glycosidic bond enables glucose to efficiently form hydrogen bonds with the Cl⁻ resulting in a lower entropy.

CONCLUSION

In this work, sugar-based DESs containing monosaccharide (glucose) and disaccharide (trehalose) as HBDs were compared to study the influence of introduction of a single covalent bond link between HBD species on behavior of deep eutectic solvents (DESs). The DSC analysis indicated significantly different glass transition temperature for the two DES systems with $DES_{(g)}$ behaving like a fluid at temperatures >50 °C, whereas $DES_{(t)}$ indicated no signs of fluid-like behavior. The simulations revealed that the glycosidic bond between sugar units in $DES_{(t)}$ hindered the free movement of trehalose, thus preventing sugar from surrounding choline chloride. The lack of movement reduced the number of interactions with choline chloride compared to glucose in $DES_{(g)}$. The QTAIM analysis revealed a significantly higher number of BCPs between choline chloride and sugar molecules in $DES_{(g)}$ compared to $DES_{(t)}$, further cementing the observation that the absence of glycosidic bond

renders flexibility to sugar molecules, leading to better interactions with choline chloride. In ${\ensuremath{\mathsf{DES}}}(g)$, a higher amount of charge transfer between choline chloride and sugar, and higher interaction energy and enthalpy of formation were observed compared to DES(t). This is a direct result of the ability of glucose molecules in $\mathsf{DES}_{(g)}$ to completely envelope choline chloride and form a significantly greater number of interactions. The entropy of formation of the DES(t) was slightly higher than that of $\mathsf{DES}_{(g)}$ as a result of fewer interactions between trehalose and choline chloride. In summary, the presence of glycosidic bond restricted the free movement of sugar, which results in a smaller number of interactions between trehalose and choline chloride. As disruption of interaction between the same molecular species is the underlying process of DES formation, the presence of the glycosidic bond between the HBD molecules results in a smaller number of interactions between sugar and choline chloride, thus significantly influencing the physical state of the DES(t) and making it behave more like a solid material, whereas $\mathrm{DES}_{(g)}$ behaves like a liquid material. Although, in this work, we used ab initio methods to describe the interactions at molecular scale that describe the short-range structure that influences the behavior of the DES, there is still scope to understand the long-range interactions that can help unravel molecular diffusion and bulk liquid structure.

SUPPLEMENTARY MATERIAL

The supplementary material contains the details of the simulation files, materials and instruments used in this work, and the general synthesis procedure for preparing DESs.

ACKNOWLEDGMENTS

This material is based on the work supported by the National Science Foundation under Grant Nos. CHE-1952846 and CHE-1919785, the Barry Goldwater Scholarship (G.I.A. and E.A.R.), and the Seidler Fellowship at Florida Gulf Coast University. The authors also acknowledge the College of Arts and Science and the high-performance computational facility at Florida Gulf Coast University for computations reported in this paper.

DATA AVAILABILITY

The data that support the findings of this study are available within the article and its supplementary material.

REFERENCES

- ¹ A. P. Abbott, D. Boothby, G. Capper, D. L. Davies, and R. K. Rasheed, "Deep eutectic solvents formed between choline chloride and carboxylic acids: Versatile alternatives to ionic liquids," J. Am. Chem. Soc. 126(29), 9142–9147 (2004).
- ²A. P. Abbott, G. Capper, D. L. Davies, R. K. Rasheed, and V. Tambyrajah, "Novel solvent properties of choline chloride/urea mixtures," Chem. Commun. **2003**(1), 70–71.
- ³ A. Hayyan, F. S. Mjalli, I. M. AlNashef, T. Al-Wahaibi, Y. M. Al-Wahaibi, and M. A. Hashim, "Fruit sugar-based deep eutectic solvents and their physical properties," Thermochim. Acta 541, 70–75 (2012).
- ⁴A. Pandey, R. Rai, M. Pal, and S. Pandey, "How polar are choline chloride-based deep eutectic solvents?," Phys. Chem. Chem. Phys. **16**(4), 1559–1568 (2014).
- ⁵A. Hayyan, F. S. Mjalli, I. M. AlNashef, Y. M. Al-Wahaibi, T. Al-Wahaibi, and M. A. Hashim, "Glucose-based deep eutectic solvents: Physical properties," J. Mol. Liq. **178**, 137–141 (2013).

- ⁶Q. Zhang, K. De Oliveira Vigier, S. Royer, and F. Jérôme, "Deep eutectic solvents: Syntheses, properties and applications," Chem. Soc. Rev. 41(21), 7108–7146 (2012).
- ⁷S. Tang, G. A. Baker, and H. Zhao, "Ether- and alcohol-functionalized task-specific ionic liquids: Attractive properties and applications," Chem. Soc. Rev. **41**(10), 4030–4066 (2012).
- ⁸P. Nockemann, B. Thijs, K. Driesen, C. R. Janssen, K. Van Hecke, L. Van Meervelt, S. Kossmann, B. Kirchner, and K. Binnemans, "Choline saccharinate and choline acesulfamate: Ionic liquids with low toxicities," J. Phys. Chem. B 111(19), 5254–5263 (2007).
- ⁹H. Zhao and G. A. Baker, "Ionic liquids and deep eutectic solvents for biodiesel synthesis: A review," J. Chem. Technol. Biotechnol. **88**(1), 3–12 (2013).
- ¹⁰J. Wu, Q. Liang, X. Yu, Q.-F. Lü, L. Ma, X. Qin, G. Chen, and B. Li, "Deep eutectic solvents for boosting electrochemical energy storage and conversion: A review and perspective," Adv. Funct. Mater. 31(22), 2011102 (2021).
- ¹¹L. L. Sze, S. Pandey, S. Ravula, S. Pandey, H. Zhao, G. A. Baker, and S. N. Baker, "Ternary deep eutectic solvents tasked for carbon dioxide capture," ACS Sustainable Chem. Eng. 2(9), 2117–2123 (2014).
- 12 L. Liu, J. Yang, J. Li, J. Dong, D. Šišak, M. Luzzatto, and L. B. McCusker, "Ionothermal synthesis and structure analysis of an open-framework zirconium phosphate with a high $\rm CO_2/CH_4$ adsorption ratio," Angew. Chem., Int. Ed. $\bf 50(35)$, 8139–8142 (2011).
- ¹³D. V. Wagle, H. Zhao, and G. A. Baker, "Deep eutectic solvents: Sustainable media for nanoscale and functional materials," Acc. Chem. Res. 47(8), 2299–2308 (2014).
- ¹⁴N. Tian, Z.-Y. Zhou, N.-F. Yu, L.-Y. Wang, and S.-G. Sun, "Direct electrode-position of tetrahexahedral Pd nanocrystals with high-index facets and high catalytic activity for ethanol electrooxidation," J. Am. Chem. Soc. 132(22), 7580–7581 (2010).
- ¹⁵M. C. Gutiérrez, F. Rubio, and F. del Monte, "Resorcinol-formaldehyde polycondensation in deep eutectic solvents for the preparation of carbons and carbon–carbon nanotube composites," Chem. Mater. 22(9), 2711–2719 (2010).
- ¹⁶M. Pal, R. Rai, A. Yadav, R. Khanna, G. A. Baker, and S. Pandey, "Self-aggregation of sodium dodecyl sulfate within (choline chloride + urea) deep eutectic solvent," Langmuir 30(44), 13191–13198 (2014).
- ¹⁷D. Carriazo, M. C. Serrano, M. C. Gutiérrez, M. L. Ferrer, and F. del Monte, "Deep-eutectic solvents playing multiple roles in the synthesis of polymers and related materials," Chem. Soc. Rev. 41(14), 4996–5014 (2012).
- ¹⁸ A. Das, S. Das, and R. Biswas, "Density relaxation and particle motion characteristics in a non-ionic deep eutectic solvent (acetamide + urea): Time-resolved fluorescence measurements and all-atom molecular dynamics simulations," J. Chem. Phys. 142(3), 034505 (2015).
- ¹⁹A. Das and R. Biswas, "Dynamic solvent control of a reaction in ionic deep eutectic solvents: Time-resolved fluorescence measurements of reactive and non-reactive dynamics in (choline chloride + urea) melts," J. Phys. Chem. B **119**(31), 10102–10113 (2015).
- ²⁰B. B. Hansen, S. Spittle, B. Chen, D. Poe, Y. Zhang, J. M. Klein, A. Horton, L. Adhikari, T. Zelovich, B. W. Doherty, B. Gurkan, E. J. Maginn, A. Ragauskas, M. Dadmun, T. A. Zawodzinski, G. A. Baker, M. E. Tuckerman, R. F. Savinell, and J. R. Sangoro, "Deep eutectic solvents: A review of fundamentals and applications," Chem. Rev. 121(3), 1232–1285 (2021).
- ²¹ D. V. Wagle, L. Adhikari, and G. A. Baker, "Computational perspectives on structure, dynamics, gas sorption, and bio-interactions in deep eutectic solvents," Deep Eutectic Solvents 448, 50–58 (2017).

- ²²H. Sun, Y. Li, X. Wu, and G. Li, "Theoretical study on the structures and properties of mixtures of urea and choline chloride," J. Mol. Model. **19**(6), 2433–2441 (2013).
- ²³O. S. Hammond, D. T. Bowron, and K. J. Edler, "Liquid structure of the choline chloride-urea deep eutectic solvent (reline) from neutron diffraction and atomistic modelling," Green Chem. **18**(9), 2736–2744 (2016).
- ²⁴S. L. Perkins, P. Painter, and C. M. Colina, "Molecular dynamic simulations and vibrational analysis of an ionic liquid analogue," J. Phys. Chem. B **117**(35), 10250–10260 (2013).
- ²⁵D. V. Wagle, G. A. Baker, and E. Mamontov, "Differential microscopic mobility of components within a deep eutectic solvent," J. Phys. Chem. Lett. **6**(15), 2924–2928 (2015).
- ²⁶G. García, M. Atilhan, and S. Aparicio, "An approach for the rationalization of melting temperature for deep eutectic solvents from DFT," Chem. Phys. Lett. 634, 151–155 (2015).
- ²⁷J. M. Rimsza and L. R. Corrales, "Adsorption complexes of copper and copper oxide in the deep eutectic solvent 2:1 urea-choline chloride," Comput. Theor. Chem. 987, 57–61 (2012).
- ²⁸C. Zhang, Y. Jia, Y. Jing, H. Wang, and K. Hong, "Main chemical species and molecular structure of deep eutectic solvent studied by experiments with DFT calculation: A case of choline chloride and magnesium chloride hexahydrate," J. Mol. Model. 20(8), 2374 (2014).
- ²⁹Y. Zhao and D. G. Truhlar, "Density functionals with broad applicability in chemistry," Acc. Chem. Res. **41**(2), 157–167 (2008).
- ³⁰S. F. Boys and F. Bernardi, "The calculation of small molecular interactions by the differences of separate total energies. Some procedures with reduced errors," Mol. Phys. **19**(4), 553–566 (1970).
- ³¹S. Grimme, "Semiempirical GGA-type density functional constructed with a long-range dispersion correction," J. Comput. Chem. **27**(15), 1787–1799 (2006).
- ³² M. J. Frisch, G. W. Trucks, H. B. Schlegel, G. E. Scuseria, M. A. Robb, J. R. Cheeseman, G. Scalmani, V. Barone, G. A. Petersson, H. Nakatsuji, X. Li, M. Caricato, A. V. Marenich, J. Bloino, B. G. Janesko, R. Gomperts, B. Mennucci, H. P. Hratchian, J. V. Ortiz, A. F. Izmaylov, J. L. Sonnenberg, D. Williams-Young, F. Ding, F. Lipparini, F. Egidi, J. Goings, B. Peng, A. Petrone, T. Henderson, D. Ranasinghe, V. G. Zakrzewski, J. Gao, N. Rega, G. Zheng, W. Liang, M. Hada, M. Ehara, K. Toyota, R. Fukuda, J. Hasegawa, M. Ishida, T. Nakajima, Y. Honda, O. Kitao, H. Nakai, T. Vreven, K. Throssell, J. A. Montgomery, Jr., J. E. Peralta, F. Ogliaro, M. J. Bearpark, J. J. Heyd, E. N. Brothers, K. N. Kudin, V. N. Staroverov, T. A. Keith, R. Kobayashi, J. Normand, K. Raghavachari, A. Rendell, J. Burant, S. Iyengar, J. Tomasi, M. Cossi, J. M. Millam, M. Klene, C. Adamo, R. Cammi, J. W. Ochterski, R. L. Martin, K. Morokuma, O. Farkas, J. B. Foresman, and D. J. Fox, Gaussian 16 C.0.1, Gaussian, Inc., Wallingford, CT, 2016.
- ³³T. Lu and F. Chen, "Multiwfn: A multifunctional wavefunction analyzer," J. Comput. Chem. 33(5), 580-592 (2012).
- ³⁴R. Dennington, T. A. Kieth, and J. M. Millam, GaussView, Semichem, Inc., Shawnee Mission, KS, 2016.
- ³⁵D. V. Wagle, C. A. Deakyne, and G. A. Baker, "Quantum chemical insight into the interactions and thermodynamics present in choline chloride based deep eutectic solvents," J. Phys. Chem. B **120**(27), 6739–6746 (2016)
- ³⁶G. V. Gibbs, O. Tamada, M. B. Boisen, and F. C. Hill, "Laplacian and bond critical point properties of the electron density distributions of sulfide bonds: A comparison with oxide bonds," Am. Mineral. 84(3), 435–446 (1999).